Vegetation mapping in drained peatlands for the carbon research objectives: a case study from Kaliningrad Region

Maxim Napreenko[1], Aleksandr Danchenkov[1],
Tatiana Napreenko-Dorokhova[1,2], Amalj Samerkhanova[1]

[1] Immanuel Kant Baltic Federal University, Kaliningrad, Russia
[2] Shirshov Institute of Oceanology, Russian Academy of Sciences, Moscow, Russia

SUMMARY

This article describes the vegetation mapping procedure adopted for the Rosyanka Carbon Supersite in Kaliningrad Province (Russia). To achieve the research objectives of the Carbon Supersite Programme which include the assessment of greenhouse gas (GHG) emissions, monitoring of ecosystem changes and modelling of the rewetting process, a detailed basemap of vegetation is required. The GIS-based vegetation map prepared includes over 100 polygon features assigned to 28 vegetation classification units comprising 6 vegetation types and 22 plant community categories, the latter approximating to associations. The mapped phytosociological units can be converted to ecology-based ones which can be used, in combination with additional data, to assign GHG flux values to the mapped units and thus to assess emission/sequestration rates at different peatland sites. Thus, the results of our investigation provide options for developing GHG flux estimation methodologies, e.g. GEST approach or 'vegetation - water level proxy' approach. We also outline possibilities for further applications of the vegetation map in relation to carbon supersite purposes. The fine-scale geobotanical map provides high-resolution cartographic material that can be correlated to land cover classes in other types of vegetation cover maps that may be required for research relating to peatland restoration, and the mapped phytosociological units may serve as a basis for increasing resolution to reveal further detail of the spatial heterogeneity of the vegetation cover.

KEY WORDS: carbon supersite, GEST, GHG flux, remote sensing, spatial heterogeneity, vegetation class

INTRODUCTION

Drained peatlands are characteristic of today's anthropogenic landscape in the detached Kaliningrad oblast (province or region) of Russia. Peatland reclamation began here during the early 19th century and its history is similar to that of nearby countries around the Baltic Sea. From the 1950s to the 1980s a large-scale peatland drainage campaign that encompassed the Baltic countries (Estonia, Latvia, Lithuania), Belarus and north-western regions of Russia including Kaliningrad resulted in the conversion of many natural mires to milled peat extraction sites. When these were abandoned for economic reasons in the 1990s, some of the disturbed peatlands became 'hotspots' for greenhouse gas (GHG) emissions, fire risk and biodiversity loss.

Mires should occupy more than 10 % of the territory of Kaliningrad Oblast (Katz 1971) but their historical conversion to farmland, forestry and peat extraction means the percentage cover of peatland for the province does not exceed 5–6 % nowadays (Napreenko 2002, 2015). On the other hand, the total area of natural and disturbed mires is still significant. Moreover, drained peatlands in Kaliningrad Oblast share environmental challenges with peatlands in nearby countries that have successful experience of mire restoration, and are similarly regarded as candidate sites for rewetting. In 2018, two pilot peatland areas in Kaliningrad were designated for ecological rehabilitation within the PeatRus Project (Napreenko *et al*. 2021).

In 2021, Kaliningrad Oblast was included in the Carbon Supersite Programme that was launched as part of the Russian Federation's National Adaptation Plan for Climate Change (MSHE 2022). The term 'carbon supersite' ('carbon polygon' in the Russian implementation) means a monitoring area with typical regional ecosystems that are distinctively involved in the carbon cycle. The project is currently active across 17 regions of Russia with different geographical locations, landscapes and habitat types.

It is well known that mires contribute to the global biogeochemical carbon cycle by sequestering CO_2 and storing the carbon in peat (Joosten *et al.* 2012). On the other hand, disturbed peatlands are an increasing source of greenhouse gas (GHG) emissions due to degradation of the peat layer after drainage and reclamation (Couwenberg 2011), and temperate Europe is the second largest hotspot of GHG emissions from degrading peat soils globally (Joosten 2009). In view of these facts, peatlands were seen as the priority terrestrial ecosystems for development of the carbon supersite in Kaliningrad Oblast. Consequently, the Rosyanka Carbon Supersite (The Rosyanka 2022) is located on a drained peatland in the central part of the region that was chosen for its geographical location in an area of intensive mire formation within the temperate zone (Rivas-Martínez *et al.* 2011, Napreenko & Napreenko-Dorokhova 2020).

An important applied aspect of carbon supersite operation links GHG emissions with spatial units in the landscape. This approach enables researchers to quantify GHG emissions and derive estimates of total fluxes based on areal mapping. Vegetation cover is considered to be the most reliable mapping target for this purpose for several reasons (Couwenberg 2011, Couwenberg *et al.* 2011):

- plants can affect GHG emissions directly by facilitating the transport of assimilates and methane fluxes via aerenchymous shunts;
- the species composition of plant communities reflects the long-term average depth and fluctuations of the water table, which correlates with GHG fluxes;
- species composition also reflects the values of other environmental factors associated with GHG emissions such as base richness (pH), nutrient availability, soil C/N, etc.); and
- vegetation mapping techniques can provide maps at different scales and levels of resolution.

Thus, within the context of carbon supersite objectives, it is envisaged that the combination of vegetation mapping tools with GHG measurements will be a necessary instrument in the implementation of mire restoration aiming to activate the process of carbon sequestration on disturbed peatlands (Napreenko *et al.* 2018, 2021). However, despite the wide range of options that modern digital mapping and remote sensing can provide, the compilation of vegetation maps for this purpose is challenging because:

- vegetation maps can vary greatly with variations in the underlying classification criteria that arise from different approaches to vegetation classification and a rather complicated hierarchy of classification units (syntaxa) which is not always easy to demonstrate on a map;
- the content of vegetation maps also depends strongly on the choice of scale and mapped area;
- plant communities temporarily occupying disturbed habitats are often disregarded in geobotanical (phytosociological) classifications of natural vegetation, so practitioners must develop their own classification units for disturbed habitats and correlate them with the existing hierarchical systems of vegetation classification; and
- an important requirement for vegetation maps prepared for carbon supersite purposes is the need to reflect the particular habitat traits that determine the level of GHG emissions.

A possible solution is to transform geobotanical maps showing the mosaic of syntaxa into ‘ecology-based’ geobotanical ones that represent the distribution of vegetation units with a certain level of GHG emissions. In this context we have to note that most vegetation maps based on remote sensing depict so-called ‘land cover classes’ that reflect, primarily, the landscape features of an area rather than the phytosociological pattern; whereas GHG fluxes are, to a great extent, related to peculiarities of the plant community and species combination.

In this article we describe a procedure for compilation of a vegetation map that combines remote sensing opportunities with phytosociological principles based on field mapping to prepare a detailed vegetation map of the Vittgirrensky peatland and outline possibilities for its further application in the context of carbon supersite objectives.

METHODS

Study area

The Rosyanka Carbon Supersite (54.799516 °N, 21.657558 °E) is located on the disturbed peatland ‘Vittgirrensky’ in Slavsky District, 80 km east of the city of Kaliningrad. The research site lies within rolling morainic terrain (Orlyonok 2008) on a local watershed of small streams (Figure 1). The total area of the peatland is currently 122 ha. It was drained in the 1980s and was subsequently used for milled peat extraction. In the late 1990s, peat extraction ceased and the site was abandoned, allowing the development of secondary vegetation. Burnt tree trunks and charcoal residues in the uppermost peat layers indicate that the whole area is subject to occasional fires.

Field survey

Preliminary ecological studies were carried out along routes running around the edge of the peatland and crossing different parts of the study area. Visually different areas on satellite images (Google Maps 2020) were then delineated to enable evaluation of

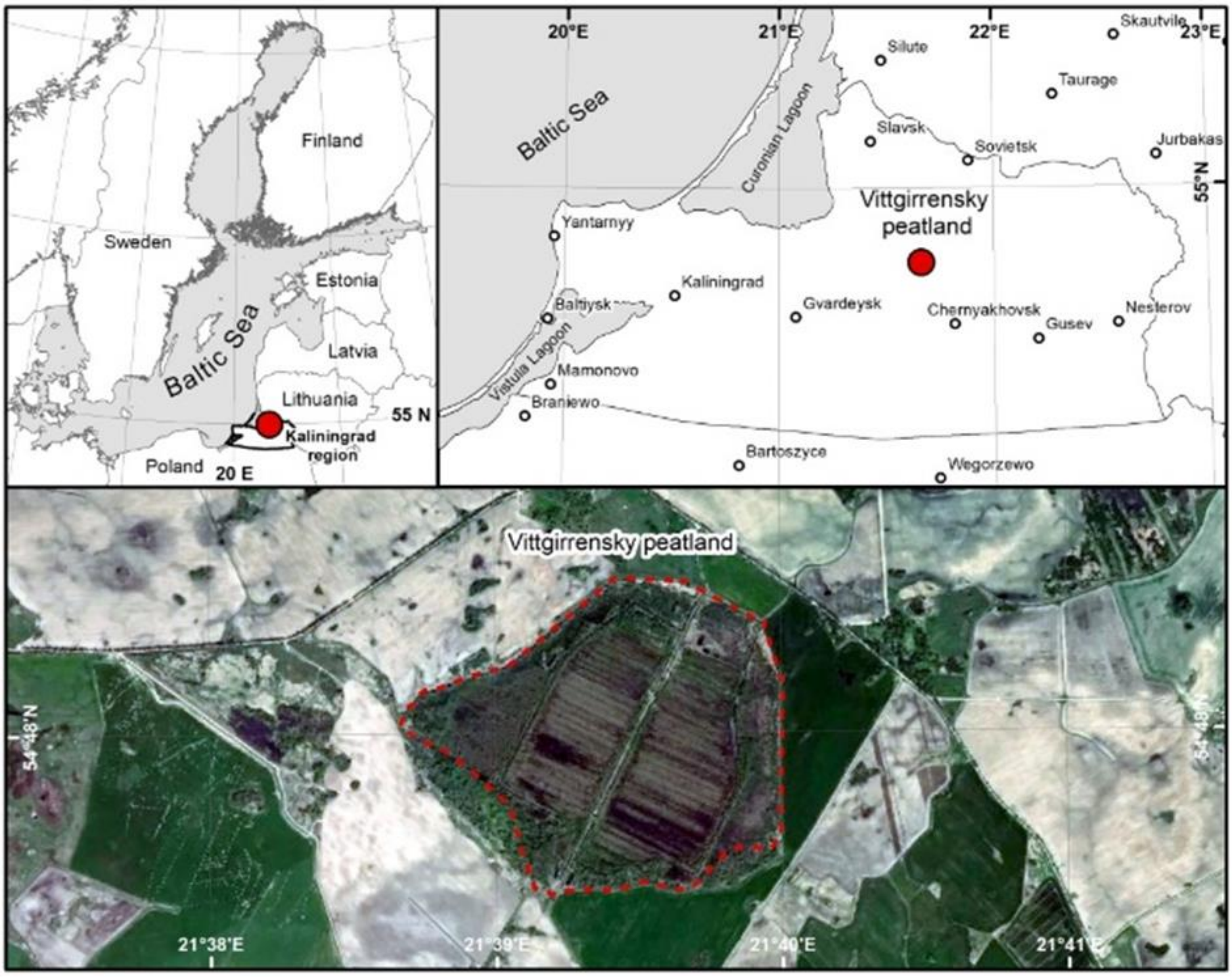

Figure 1. The geographical location of the Vittgirrensky peatland (Rosyanka Carbon Supersite). Source: Google Maps (2020).

the areal extent of different vegetation units on the peatland. The routes and preliminary vegetation unit boundaries were spatially referenced using compact GPS chart plotter receivers (Garmin eTrex10).

The detection and verification of vegetation were performed using relevé sampling (geobotanical descriptions) of permanent plots placed randomly in the most representative sites within the preliminary vegetation units. Permanent plots were established and described as frequently as the character of the plant community changed, regardless of whether or not a corresponding vegetation unit had already been delineated. In some cases we defined the borders of sites with different vegetation in the field.

The plot size was 100 m^2 (10 × 10 m) for open sites and 400 m^2 (20 × 20 m) for areas with dense tree canopies. The following traits were taken as the main indicators: plant species composition, microrelief in the plot, hydrological characteristics of the site, and traces of fire. Within the plots we recorded all plant species in each layer, along with their percentage cover which was further converted to a value on the Braun-Blanquet scale (Braun-Blanquet 1964). Specimens of bryophytes and lichens that could not be identified in the field were collected for identification under laboratory conditions. For species contributing to the tree layer we also recorded canopy cover, mean trunk diameter and height. In total, 84 relevés were recorded (see Appendix).

Microrelief in the plot and spatial heterogeneity within the identified vegetation units, as well as vegetation cover in the drainage ditches, were also recorded and described in general. These results are not discussed here because further detailed analysis requiring more relevés and imagery of higher resolution are needed. For this reason, sites with patterning (small hummocks, tussocks, wet depressions, bryophyte synusiae) were not divided into different elements for description; at the current stage of research it is not clear whether they can be distinguished as separate plant communities or are structural parts of one phytocoenosis. Nevertheless, in some cases we recorded relevés on the moss carpets within such sites using small plots ranging in area from 0.25 m^2 to 2 m^2. This was done to reveal the coverage of different bryophyte and lichen species within the sinusia. The data from the small relevés were integrated into the data for the plot.

To assess the distribution of each vegetation unit within the study area, we recorded its occurrence across the peatland. Residual peat depth and water table depth below surface were measured simultaneously in boreholes created using a Russian peat corer. For traces of fire, we recorded either percentage cover (crusts of burnt peat and pyrogenic moss carpets) or relative abundance (of burnt trunks and charcoal residues in the surface layer of peat).

The field data collected were used to correct the boundaries of the vegetation units derived from satellite images. These data provided a basis for compilation of a preliminary vegetation map (Napreenko *et al.* 2021).

Aerial imagery and digital terrain model of the peatland

To obtain detailed visual information as a basis for improving the accuracy of plant community boundaries, an aerial photography flight plan was executed using a DJI Mavic Pro drone equipped with a digital camera. Coordinates were referenced to a network of five ground control points distributed evenly over the study area (Nocerino *et al.* 2013) using an EFT M2 GNSS receiver. To ensure correct reconstruction, the drone flights were performed at an altitude of 50–70 metres over a network of profiles with an overlap of 80 % between frames, which is compliant with a resolution of 0.03 m per pixel.

To estimate elevation differences for indicative determination of plant life forms (trees, shrubs or herbs) we constructed a digital terrain model (DTM) using digital image processing techniques based on Structure-from-Motion (SfM) computer vision algorithms, which aim to reconstruct the 3D structure of the scene from correspondences in overlapping digital images (Snavely *et al.* 2008, Clapuyt *et al.* 2016). This technology enables the reconstruction of surface topography in a study area from a series of digital images captured from a UAV equipped with a consumer-grade camera, and is widely used for remote environmental observation and monitoring (Neitzel & Klonowski 2011, Clapuyt *et al.* 2016).

Vectorisation and mapping procedure

A detailed vegetation map was plotted, based on a comprehensive analysis of the preliminary vegetation map with integration of the remote sensing data and results of the additional field observations.

Raster surfaces of indicative plant life forms based on the DTM (Figure 2) were verified using the field observations. Treed areas were characterised by abrupt changes in height between canopy spot levels and ground level, as well as by increased values of absolute height. Shrub vegetation exhibited more gradual height changes, while the DTM images for herbaceous vegetation had a homogeneous appearance with insignificant height differences.

A classification of plant community categories was developed from the preliminary vegetation map and field data. The aerial photography was analysed for representative textures associated with visually derived subdivisions of vegetation sites. Each texture class was correlated with characteristic features visible in the aerial imagery and, on this basis, image fragments that displayed the most typical features were extracted (Figure 3).

The vegetation plots were then vectorised and assigned to texture classes specific to the plant community categories using ESRI ArcGIS 10.0 software. Surfaces with indicative plant life forms and field data were also analysed. Cross-validation methods were used to compare the assigned category with the category established during the field surveys. In this manner, the accuracy of classification was checked and then iteratively corrected to minimise errors and increase reliability of the results.

RESULTS

Stage 1: Preliminary vegetation map

As shown in an earlier publication (Napreenko *et al.* 2021), the preliminary vegetation map derived from satellite images and field geobotanical descriptions of the study area depicted 5 vegetation types and 17 plant community categories which almost matched the plant associations that would be described using the dominant approach to vegetation classification in Russia (Alexandrova 1969, 1971). This map showed the general distribution of vegetation types across the study area, providing a basis for estimation of the approximate sizes of different sites and the diversity of vegetation cover.

The objectives of the carbon supersite required finer scaling within some of these vegetation units to create a more detailed map delineating many small units that were not included in the preliminary map but were potentially significant in terms of GHG fluxes. To map these small units with sufficient accuracy to represent them on a digital map that could subsequently be used to calculate site areas and the corresponding GHG emissions, field verification of their boundaries was necessary.

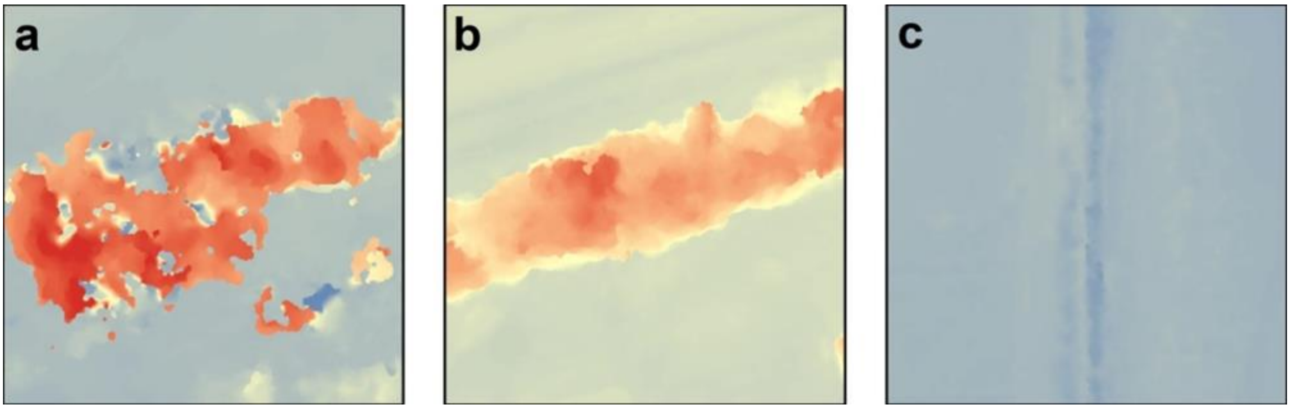

Figure 2. Typical examples of different plant life forms as represented in digital terrain model (DTM) images: (a) trees; (b) shrubs; (c) herbs.

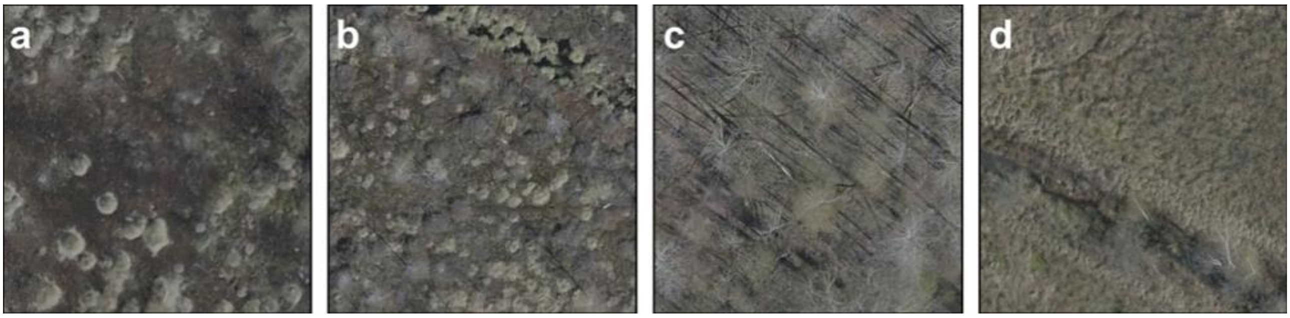

Figure 3. Fragments of the vertical aerial photography images displaying the most typical features for some plant community categories: (a) bare peat plots along trunk ditches; (b) sparse birch regrowth with *Calluna*; (c) birch and aspen wet forests; (d) *Juncus*-dominated fen-like community.

Stage 2: Detailed vegetation map

The analysis and digitisation of satellite imagery and aerial photography produced a layer of about 100 polygons (Figure 4). After ground truthing and comparison with the preliminary vegetation map (Napreenko *et al*. 2018, 2021), these polygons were classified into 22 GIS layers that were considered equivalent to 22 plant community categories, then combined into 6 types of vegetation cover to create the updated vegetation map of the carbon supersite (Figure 5). This detailed vegetation map incorporated new data, in particular:

- the distribution of bare peat (assigned as a separate vegetation type; additional localities were marked on the map);
- sites with *Phragmites* (three new categories were assigned within the type ‘Ligneous vegetation on peaty heathlands’);
- sites with different birch stand densities (one additional category was assigned); and
- ditches with different types of hydrophilic vegetation (ditches are being inventoried for vegetation cover and hydrological properties; the data will be used to generate a separate layer on the digital map).

The plant community categories and vegetation types were derived from the delineated vegetation plots, again in terms of the dominant Russian classification system (Alexandrova 1969, 1971). As in the case of the preliminary vegetation map (Napreenko *et al*. 2021), the plant community categories were, in general, close to the plant associations of classical geobotany.

Main features of present-day vegetation in the Rosyanka Carbon Supersite

The 6 vegetation types that we derived to describe the current vegetation cover of the Vittgirrensky peatland are: 1) forest arboreal vegetation, 2) ligneous coppice vegetation, 3) shrub vegetation, 4) herbaceous and dwarf-shrub vegetation, 5) sparse moss vegetation on

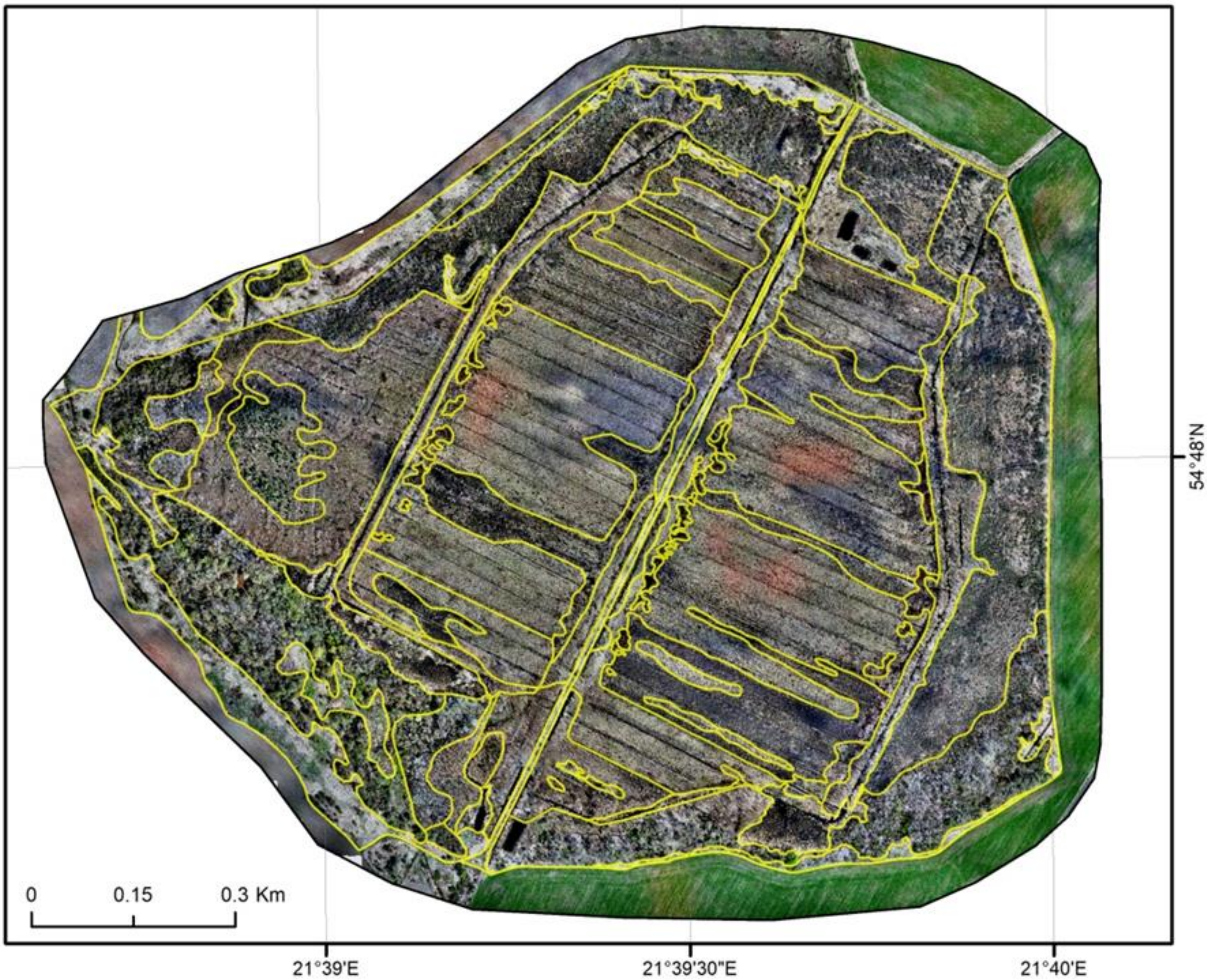

Figure 4. Map delineating the plant community categories obtained by automatic digitisation of aerial imagery of the Vittgirrensky peatland (Rosyanka Carbon Supersite).

bare peat, and 6) vegetation of hydrophilic habitats. Each type is subdivided into several of the 22 plant community categories. Arboreal vegetation (including both forest and coppice types) is most widespread across the study area and comprises 13 plant community categories. The shrub and herbaceous/dwarf-shrub types are less diverse with 3 and 4 categories, respectively. The sparse moss and hydrophilic types are each represented by only one category.

Both vegetation maps (Napreenko *et al.* 2021 and Figure 5) show that the territory of the Vittgirrensky peatland can be divided into two zones. The *central* zone is covered by peatland regrowth communities (mainly birch stand) which developed in the last 20–40 years following destruction of the primary bog vegetation. The *edge (peripheral)* zone has a longer development history of 60–70 years and is occupied by inundated forests and shrublands. Thus, the present-day vegetation of the Vittgirrensky peatland can be regarded as a recovery complex at various successional stages, developing towards tall birch stands in the centre and wet forest-shrub communities around the edges.

DISCUSSION

The objectives of the carbon supersite (especially rewetting) require a strategy based on 'ecological cartography' that converts vegetation units based on purely geobotanical classifications to units with the desired hydrological characteristics, GHG emission levels, biodiversity and fire risk. For this purpose, we have developed methodological approaches to transform phytosociological syntaxa into 'ecology-based' geobotanical units.

The future development of vegetation diversity on the Vittgirrensky peatland is expected to indicate changes in the character of GHG fluxes, and will

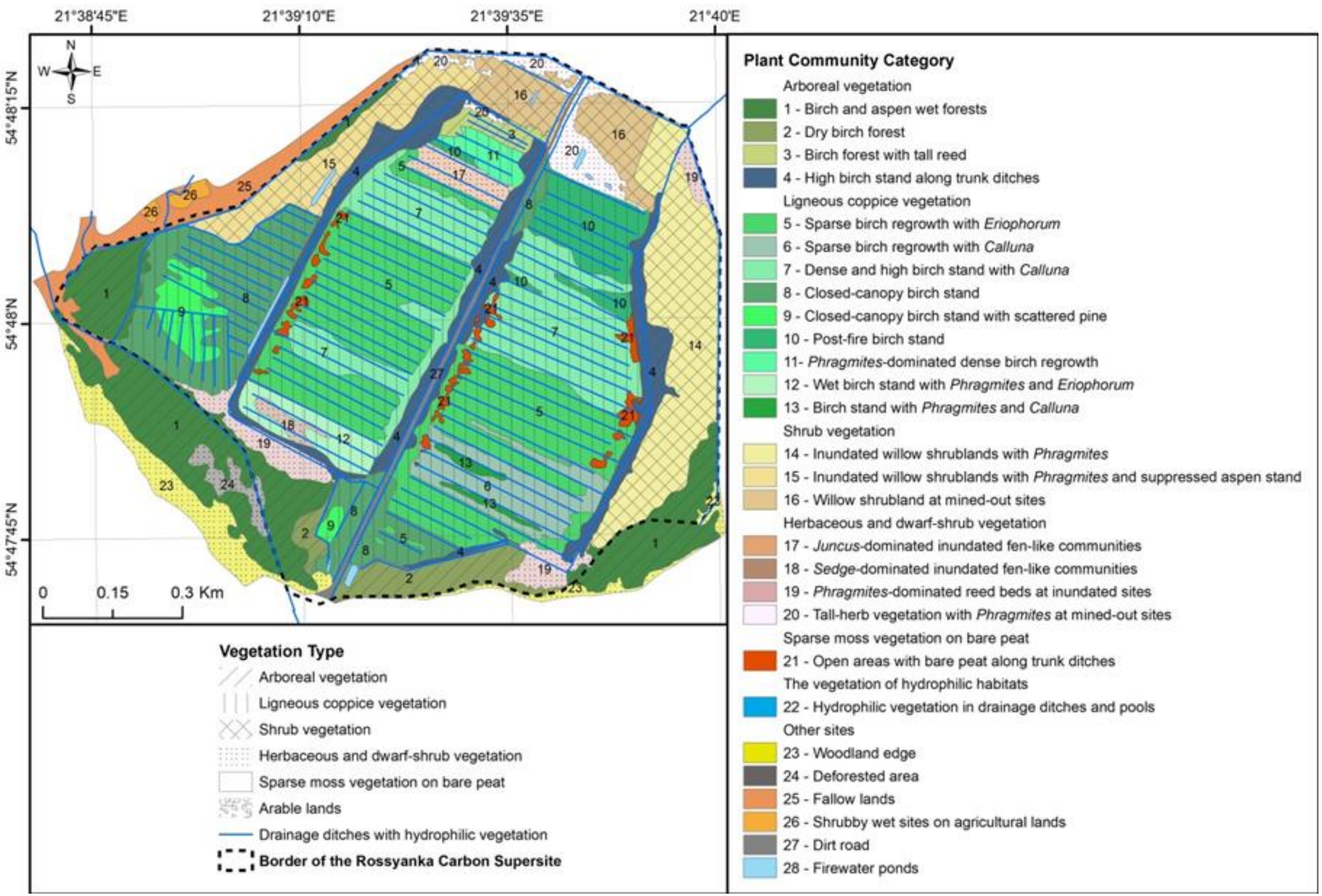

Figure 5. Detailed vegetation map of the Vittgirrensky peatland (Rosyanka Carbon Supersite).

depend on the management strategy adopted (e.g., rewetting, drainage or spontaneous development with zero intervention). The discussion that follows considers how our methodology for describing the vegetation cover compares and could be combined with other techniques, as well as the opportunities for its further development and wider application, in the context of carbon supersite goals.

Correlating geobotanical (phytosociological) units with land cover classes

Remote sensing is now widely used for vegetation mapping, which provides many options for processing and interpretation of the mapped material. In most applications of this technique, the final vegetation units are 'land cover classes' produced via cluster analysis or machine learning. The land cover classes identified are not usually described in phytosociological terms, but reflect a system of unification that enables comparisons of vegetation cover between different regions.

In contrast to the geobotanical approach described in this article, the mapping procedure does not require long-term field studies, and maps covering sufficiently large areas can be compiled quickly. At the same time, the maps obtained are quite strongly generalised, which could affect the accuracy of GHG flux estimates. In this regard, we see correlation of the mapped land cover classes with geobotanical (phytosociological) units as one of the important tasks within carbon projects on disturbed peatlands.

For the purposes of our case study, we considered the methodology for identification of land cover classes in human-disturbed peatlands that was developed by the research group of A.A. Sirin (Sirin *et al.* 2018, 2020). This procedure detects land cover units by semi-automatic machine processing of satellite images, mainly using features of the vegetation cover. For peatlands which have been disturbed by humans, the resulting units belong to one of six vegetation classes, namely: 1) 'bare peat', 2) 'grass' (herb and reed communities), 3) 'pine' (pine stands), 4) 'willow-birch' (willow- and/or birch-dominated communities), 5) 'hydrophilic communities' (reed communities with *Scirpus*, tall sedges and *Phragmites*), and 6) 'water bodies' (slightly overgrown with plants). These land cover classes are claimed to reflect the hydrological conditions and the level of GHG emissions in a habitat sufficiently to make the identification and mapping of these classes relevant to the planning of rewetting management and mire rehabilitation.

At the current stage of our research at Vittgirrensky, we were able to compile a map of these land cover classes on the basis of geobotanical characteristics of the vegetation units without utilising satellite imagery. The map (Figure 6) was generated semi-automatically, using GIS tools, from the detailed vegetation map of the Vittgirrensky peatland, by allocating one or more of the geobotanical units to each of the six land cover classes. Table 1 shows how the geobotanical units were matched to the defined land cover classes.

Figure 6 shows that most of the Vittgirrensky Peatland is occupied by sites of class 4 ('communities with willow and/or birch') but, as can be seen from Table 1, it unites plant communities of various types with different structures and hydrology. Such generalisation is likely to limit the usefulness of the land cover map for carbon supersite purposes.

The map thus derived is relevant to the assessment of degree of disturbance in a peatland abandoned after peat extraction, the identification of priority rewetting and measurement sites, and for monitoring changes during rewetting operations; and its most important advantage is that the data can be easily compared with data recorded in other regions. However, this land cover map lacks sufficient detail to be useful as a basis for modelling the dynamics of GHG fluxes. The necessary differentiation of land cover classes could be achieved by combining this map with detailed geobotanical cartography, and the combined map might then form a basis for further measurements of water table depth, GHG fluxes, peat deposits, etc.

Linking cartographic data to GHG emission proxies using different estimation approaches

Vegetation is often considered to serve as a reliable proxy for GHG flux estimation because its structure, species composition and traits are strongly correlated with the environmental factors affecting GHG emissions (Couwenberg *et al.* 2011, Liu *et al.* 2020). Repeated vegetation mapping can, therefore, provide sufficient information to infer changes in GHG emission rates. Two approaches have been developed and are considered below.

The GEST approach and its regional calibration across the temperate zone in Central Europe

The concept of Greenhouse Gas Emission Site Types (GESTs) is the most practical and well-known methodology for identifying sites with different levels of GHG emissions. It was developed at the University of Greifswald for wetland vegetation, primarily in disturbed peatlands (Couwenberg *et al.* 2008, Tiele *et al.* 2009, Couwenberg 2011). The GEST system is based on a concept of 'vegetation form' (Koska *et al.* 2001) that regards plant species and their associations, being confined to certain

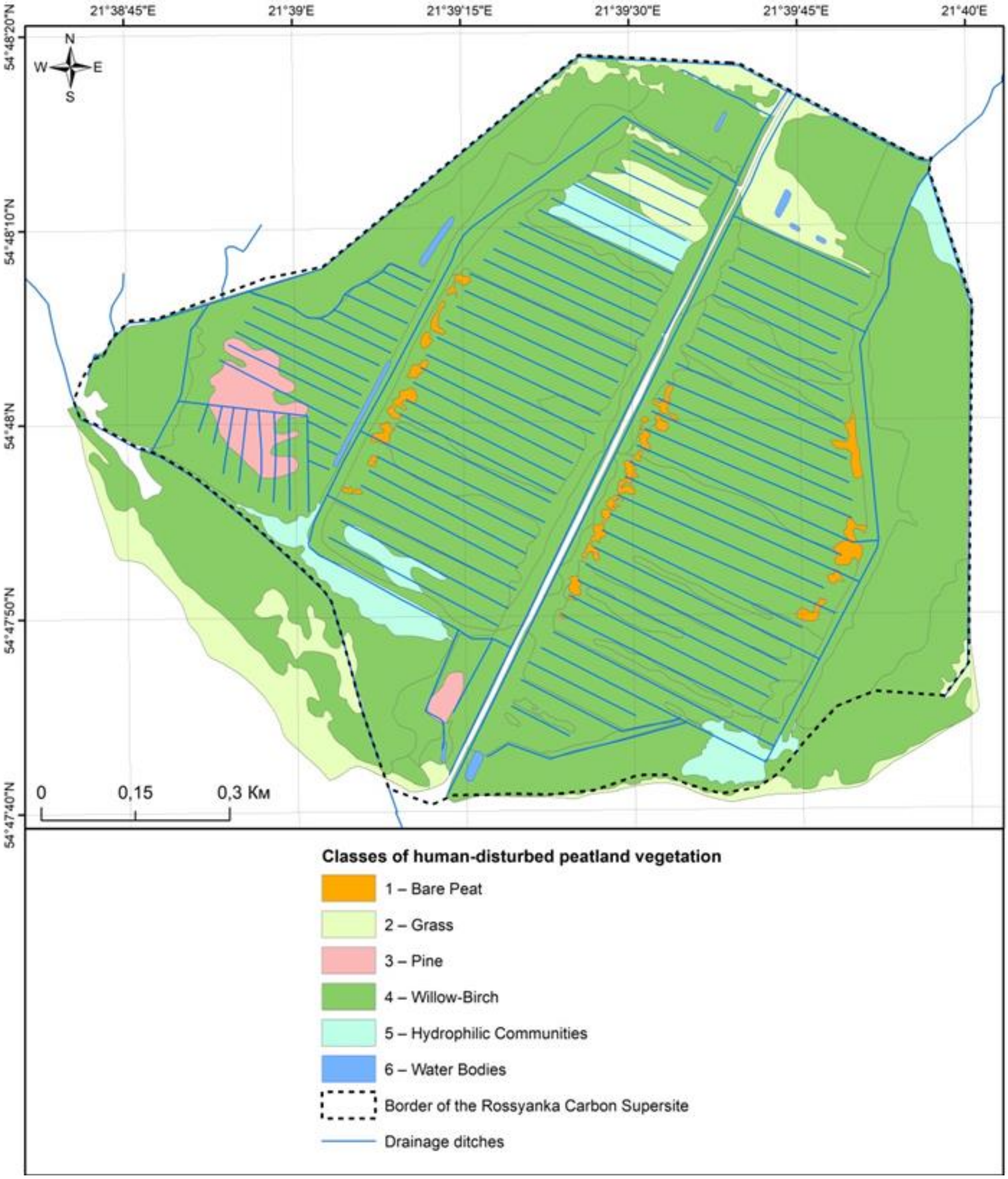

Figure 6. Land cover classes of human-disturbed peatland vegetation identified for the Vittgirrensky Peatland (Rosyanka Carbon Supersite).

Table 1. Correlation between plant community categories from the detailed vegetation map of the Vittgirrensky peatland (Figure 5) and the land cover classes of human-disturbed peatland vegetation (Figure 6).

Land Cover Class	Plant Community Category	Area (ha)	
Bare Peat	(21) Open areas with bare peat along trunk ditches	1.29	1.29
Grass	(11) *Phragmites*-dominated dense birch regrowth	1.08	9.03
	(20) Tall-herb vegetation with *Phragmites* at mined-out sites	2.84	
	(23) Woodland edge	4.25	
	(24) Deforested area	0.86	
Pine	(9) Closed-canopy birch stand with scattered pine	2.30	2.30
Willow-Birch	(1) Birch and aspen wet forest	15.92	108.72
	(2) Dry birch forest	3.71	
	(3) Birch forest with tall reed	0.96	
	(4) High birch stand along trunk ditches	9.90	
	(5) Sparse birch regrowth with *Eriophorum*	21.98	
	(6) Sparse birch regrowth with *Calluna*	4.32	
	(7) Dense and high birch regrowth with *Calluna*	13.82	
	(8) Closed-canopy birch stand	11.42	
	(10) Post-fire birch stand	4.29	
	(12) Wet birch stand with *Phragmites* and *Eriophorum*	1.93	
	(13) Birch stand with *Phragmites* and *Calluna*	0.56	
	(14) Inundated willow shrublands with *Phragmites*	10.57	
	(15) Inundated willow shrublands with *Phragmites* and suppressed aspen stand	4.61	
	(16) Willow shrubland at mined-out sites	4.73	
Hydrophilic Communities (including drainage ditches*)	(17) *Juncus*-dominated inundated fen-like communities	1.29	4.82
	(18) Sedge-dominated inundated fen-like communities	0.50	
	(19) *Phragmites*-dominated reed beds at inundated sites	3.03	
	(22) Hydrophilic vegetation in drainage ditches and pools	≈ 5.3**	
Water Bodies	(28) Firewater ponds	0.40	0.40
Other Areas (not included in our considerations)	(25) Fallow land	4.22	
	(26) Shrubby wet sites on agricultural land	0.41	
	(27) Dirt road	0.93	

* Drainage ditches are not identified as a separate land cover class within the classification (Sirin *et al.* 2018, 2020), but this question is under discussion (Waddington & Day 2007, Couwenberg *et al.* 2008, Sirin *et al.* 2012, 2018); ** as linear features on the map, the drainage ditches were excluded from the area calculation, but we estimate that their total area is more than 5 ha (which should be subtracted from the areas of other patches).

ranges along a gradient of a given abiotic factor, as good indicators of the site conditions. Such indirect assessment of GHG fluxes is less expensive than direct measurement but requires a long period of field studies at research sites using a standardised measurement protocol for GHG emissions with simultaneous monitoring of related environmental factors (Couwenberg *et al.* 2008, Couwenberg 2011). The emissions data obtained are assumed to be relevant to other sites with comparable vegetation cover (with a specific group of indicator species) in regions with similar climate and vegetation.

The GEST methodology enables not only the estimation of GHG fluxes in a study area but also predictions of future developments of the situation under different scenarios. At the same time, there are a number of restrictions that limit its application at large scale. Among these are the need for long-term field measurements, the absence of a unified GEST classification and GEST catalogue, and the regional limitation on data relevance. Nevertheless, we envisage good potential for application of the GEST approach within the carbon supersite programme in Kaliningrad Region, as well as some options for further development of the methodology based on the results of our investigations.

The GEST methodology has been tested in some parts of central Europe, primarily in north-eastern Germany and Belarus (Tiele *et al.* 2009, Couwenberg *et al.* 2011), where it has generally shown good results based on long-term GHG flux measurements and water level monitoring. Given that Kaliningrad Region is located in the same bioclimatic zone of temperate Europe with similar zonal vegetation (Rivas-Martínez *et al.* 2011, Napreenko & Napreenko-Dorokhova 2020) and similar mean annual temperature and precipitation, it should be feasible to extend the GEST approach into this region with appropriate supporting calibration studies.

Special investigations devoted to the flora and vegetation of mires in Kaliningrad Region (Napreenko 2002, 2015) have shown that they are close in character to mires in other temperate parts of central Europe (Yurkovskaya 1980, Jiroušek *et al.* 2022) including north-eastern Germany (Jeschke *et al.* 2001) and Belarus (Grummo *et al.* 2009). This is also reflected by the similar structure of 'vegetation forms' used within the GEST procedure. As shown in Table 2, some of the plant community categories identified on the vegetation map in Figure 5 are compliant with GEST units ('vegetation type' or 'vegetation form') described from north-eastern Germany and/or Belarus. For other vegetation units we see similar structure to northern German or Belarussian GEST units but certain departures from their typical species composition according to available descriptions (Couwenberg *et al.* 2008, Couwenberg 2011). Nonetheless, their GHG emission levels may be similar. On the other hand, some plant community categories in the Vittgirrensky peatland (e.g., 'hydrophilic habitats' (22), 'open areas with bare peat' (21), and categories 5–13 within the 'ligneous coppice vegetation' type) may have been subdivided into separate units to comply with the different vegetation forms occurring in other locations. A similar subdivision for the 'bare peat' type is applied in Belarus (Couwenberg *et al.* 2011). Also, some 'plant community categories', e.g. units of 'ligneous coppice vegetation type', have been identified as new 'vegetation forms' here, but still require validation by the panel of regional experts.

At this stage the 'plant community categories' that have been distinguished may be regarded only as potential 'vegetation forms' for application of the GEST technique on disturbed peatland, because the final elaboration of GESTs will be possible only after several water level and GHG measurement campaigns. We must also note that the elaboration of potential GESTs within our relatively small study area is based on a limited number of the full suite of vegetation forms that are typical for drained and disturbed peatland.

The list of GESTs for Kaliningrad Region can be extended by adding units identified using the vegetation forms on undisturbed mires. The first data were obtained from an assessment of GHG emissions on the large (2600 ha) Zehlau raised bog. The resulting map of vegetation cover units covered the whole area of the mire (Schwill *et al.* 2010a) and the 'vegetation forms' identified were: *Eriophorum* - *Pinus* - wood, *Eriophorum* - *Betula* - wood, *Pinus* - *Sphagnum* - lawn, *Sphagnum* - *Utricularia* - *Phragmites* - lawn, green *Eriophorum* - *Sphagnum* - lawn, green *Sphagnum* - hollow, green *Sphagnum* - hollow with flark complex, and red *Sphagnum* - lawn (Schwill *et al.* 2010a). Most of these units are typical for undisturbed bogs and uncommon in the drained peatland on peat extraction sites, but can be considered at the stage of planning rewetting scenarios. As the scope of the Zehlau project did not include regional calibration of 'vegetation forms', CO_2/CH_4 emission values from north-eastern Germany were assigned (as approximations) to the mapped 'vegetation forms' to enable a rough calculation of the total annual GHG emissions, and on this basis two future scenarios were explored (Schwill *et al.* 2010a, 2010b).

Table 2. Comparison of the 'vegetation types' on drained peatlands in north-eastern Germany according to Koska *et al.* (2001) and Couwenberg *et al.* (2008), and in Belarus after Couwenberg *et al.* (2011), with the potentially equivalent 'plant community categories' in the Vittgirrensky peatland, Kaliningrad Region (see Figure 5). The typical/characteristic species are given below the name of each vegetation type/form.

No.	NE Germany: vegetation types and vegetation forms (with codes)	Belarus: vegetation types*	Kaliningrad Region: plant community categories
2	Moderately moist forbs & meadows *Urtica dioica* *Cirsium* spp. *Galium* spp.	Moderately moist forb meadows *Elytrigia repens* *Urtica dioica* *Bidens frondosa*	-
3	Moist forbs & meadows *Phragmites australis* *Cirsium* spp. *Urtica dioica* *Lythrum salicaria*	Moist forb meadows *Phalaris arundinacea* *Ranunculus repens* *Juncus effusus* *Agrostis* spp.	Tall-herb vegetation with *Phragmites* (20) *Phragmites australis* *Calamagrostis lanceolata* *Solidago canadensis*
4	Moist bog heath *Calluna vulgaris* *Vaccinium myrtillus* *Ledum palustre* *Dicranum scoparium* *Pleurozium schreberi*	Moist bog heath *Eriophorum vaginatum* *Calluna vulgaris* *Betula* spp.	Categories 5-10 within 'Ligneous coppice vegetation type' *Eriophorum vaginatum* *Calluna vulgaris* *Betula* spp.
5	Moist bare peat	Bare peat	Open sites with bare peat (21)
6	-	*Bare peat with *Polytrichum* *Polytrichum strictum* *Funaria hygrometrica* *Calluna vulgaris* *Eriophorum vaginatum* *Betula pendula*	Open sites with bare peat (21**) *Polytrichum strictum*
7	-	*Bare peat with *Calluna* *Calluna vulgaris*	-
8	-	*Bare peat with *Eriophorum* *Eriophorum vaginatum*	-
12	Very moist bog heath *Calluna vulgaris* *Vaccinium myrtillus* *Ledum palustre* *Sphagnum* spp.	Very moist bog heath *Calluna vulgaris* *Eriophorum vaginatum* *Ledum palustre* *Chamaedaphne calyculata* *Polytrichum strictum* *Pleurozium schreberi* *Sphagnum angustifolium* *Pinus sylvestris*	-
15	Very moist peat moss lawn, *Sphagnum* lawn with large *Eriophorum* tussocks (Ml1d) *Sphagnum recurvum agg.**** *Eriophorum vaginatum*	-	Hydrophilic vegetation in drainage ditches and pools (22****) *Sphagnum. cuspidatum* *Eriophorum vaginatum*

No.	NE Germany: vegetation types and vegetation forms (with codes)	Belarus: vegetation types*	Kaliningrad Region: plant community categories
18	Wet short and tall sedge marshes / reeds with moss layer, *Sphagnum*-*Carex* - *Eriophorum* - marsh (sS2) *Eriophorum angustifolium* *Carex nigra* *C. curta* *Sphagnum recurvum agg.****	-	Sedge-dominated inundated fen-like communities (18) *Eriophorum vaginatum* *Carex acuta* *Phragmites australis* *Juncus effusus* *Sphagnum fallax* *S. angustifolium* *Betula* spp.
19	Wet short & tall sedge marshes & reeds with moss layer, *Sphagnum* - *Juncus effusus* - marsh (tS1) *Juncus effusus* *Sphagnum recurvum agg.****	-	*Juncus*-dominated inundated fen-like communities (17) *Juncus effusus* *Sphagnum cuspidatum* *S. angustifolium* *S. teres*
20	Wet tall reeds *Sphagnum* - *Phragmites* - reeds (tR5) *Phragmites australis* *Solanum dulcamara*	Wet reeds and sedge fens-	*Phragmites*-dominated reed beds at inundated areas (19) *Phragmites australis* *Carex acuta*
21	Wet peat moss lawn green *Sphagnum* lawn (Ml2) *Sphagnum recurvum agg.****	Wet *Sphagnum* lawn, *Sphagnum angustifolium* *S. cuspidatum*	Hydrophilic vegetation in drainage ditches and pools (22****) *Sphagnum cuspidatum* *Eriophorum vaginatum*

* The ‘bare peat’ vegetation types on Belarussian peatlands should be regarded as types of ‘vegetation form’ as they seem to be variants (with similar structure) of one type of vegetation cover, according to the description provided by Couwenberg *et al.* (2011).

** The variant with sparse moss vegetation, which is not yet mapped as a distinct category.

*** The name ‘*Sphagnum recurvum* agg.’ is used for a trio of closely related *Sphagnum* species, namely *S. angustifolium, S. fallax* and *S. flexuosum*, which can be easily confused in the field (Daniels & Eddy 1985, Dierßen 1996, Ignatov & Ignatova 2003). In the context of the investigated site the species most likely to be allocated to this taxon are, apparently, *S. angustifolium* and/or *S. fallax*.

**** The variant with *Sphagnum cuspidatum/angustifolium* and *Eriophorum* tussocks, which is not yet mapped as a distinct category.

The ‘vegetation-water level proxy’ approach

This approach combines the bioindication of water level by vegetation types and the correlation of water level with GHG emissions (Liu *et al*. 2020). The main difference from GEST methodology is that, instead of using characteristic plant species as indicators of site factors including water level, this concept uses indicator value classifications (Ellenberg *et al*. 1992, Koska *et al*. 2001) to directly link local vegetation types to measured mean water levels. GHG fluxes are calculated, without direct measurements, via regression models based on meta-analysis of year-round flux data collected in temperate Europe. The approach was demonstrated in a case study on a rewetted fen in The Netherlands by Liu *et al*. (2020), who emphasise the applicability and cost-efficiency of the method under location-specific conditions, and especially for monitoring the effects of management practices and rewetting projects.

It is important that repeated detailed vegetation mapping based on the dominant plant communities is undertaken at an early stage (as in the GEST-focused investigation reported here). Combining these data with mean values of measured water levels and estimates of GHG fluxes can provide spatially explicit information about GHG emissions from the study area. A second important issue relates to avoiding any need for troubleshooting during the GHG flux estimations by increasing map resolution to enable the separation of appropriate landscape units.

Map resolution

Vegetation pattern and complexity of micro-relief are inherent traits of bog habitats that should be taken into consideration when mapping vegetation for carbon supersite purposes, as the differences in GHG fluxes between pattern elements within the same vegetation unit could be vital to the accuracy of calibration. Incorporating this complexity into map units for the Vittgirrensky peatland was not totally straightforward, as discussed below.

Structural heterogeneity within a vegetation unit

Carbon fluxes at landscape scale are strongly dependent on spatial heterogeneity and diversity (Premke *et al*. 2016) in terms of both botanical composition and site structure. For example, in the 'bare peat' category (21 in Figure 5), one can distinguish patches of: 1) unchanged loose peat, 2) peat surface affected by fire (with a crust of burnt peat), and 3) patches of peat partially covered with *Polytrichum* (Figure 7).

Similar conditions may arise locally within other vegetation units, so patches of 'bare peat' may be found in sites that belong to other vegetation types. Our field investigations confirmed this thesis for the Vittgirrensky peatland where, for example, patches of bare peat with sparse *Polytrichum* (variant of the 'open sites with bare peat' category) may occur in several distinct sites (plant community categories) such as 'sparse birch regrowth with *Eriophorum*' (5 in Figure 5), 'post-fire birch stand' (10 in Figure 5) as well as the 'open areas with bare peat' category (21 in Figure 5). In the first of these, the patches of bare peat occur between cottongrass tussocks (Figure 8a) while in the second they are the main components of the surface beneath the tree layer (Figure 8b) and in the third (treeless) site they have only minor coverage (Figure 8c).

These structural peculiarities may require more detailed calibration using ultra-fine-scale mapping of vegetation cover, which would be a labour-intensive long-term procedure as it is hardly feasible without detailed on-site verification. However, it may be possible to sufficiently improve the reliability of emission values by estimating spatial heterogeneity for such complex vegetation units.

Figure 7. Heterogeneity of the vegetation cover within a single plant community category ('bare peat'): 1) unchanged loose peat surface, 2) crust of burnt peat, 3) patches of peat with partial cover of *Polytrichum* (photo: M. Napreenko).

Integrating the diversity of ditches into the GEST procedure

GESTs are not usually elaborated for drainage ditches (Couwenberg *et al.* 2008) because their total area is a very small fraction of the area of the whole peatland. However, recent investigations on drained peatlands in European Russia (Waddington & Day 2007, Sirin *et al.* 2012) have detected rather high methane emissions from drainage ditches. This significant GHG flux must be taken into account when assessing GHG emissions from disturbed peatlands as well as during the elaboration of GESTs.

Our first botanical studies in the Vittgirrensky peatland revealed various types of melioration canals (Figure 9) that vary in structure and are occupied by different vegetation (Napreenko *et al.* 2018, 2021). These factors may affect the GHG effluxes from ditches (Waddington & Day 2007, Sirin *et al.* 2012). We consider that the vegetation cover is a good ecological indicator for this habitat type and, therefore, propose that the drainage ditches should be included in the classification of vegetation cover and be treated as a separate classification unit for vegetation mapping and further ecological measurements. Taking into account the different structures of ditches, we expect they will be referred to as various 'vegetation forms'.

Potential for upscaling

Vegetation mapping is clearly a crucial tool in the GEST method and the 'vegetation-water level' approach. Moreover, both of these approaches were developed, and are therefore valid, within the temperate zone of Europe; and are based on an idea

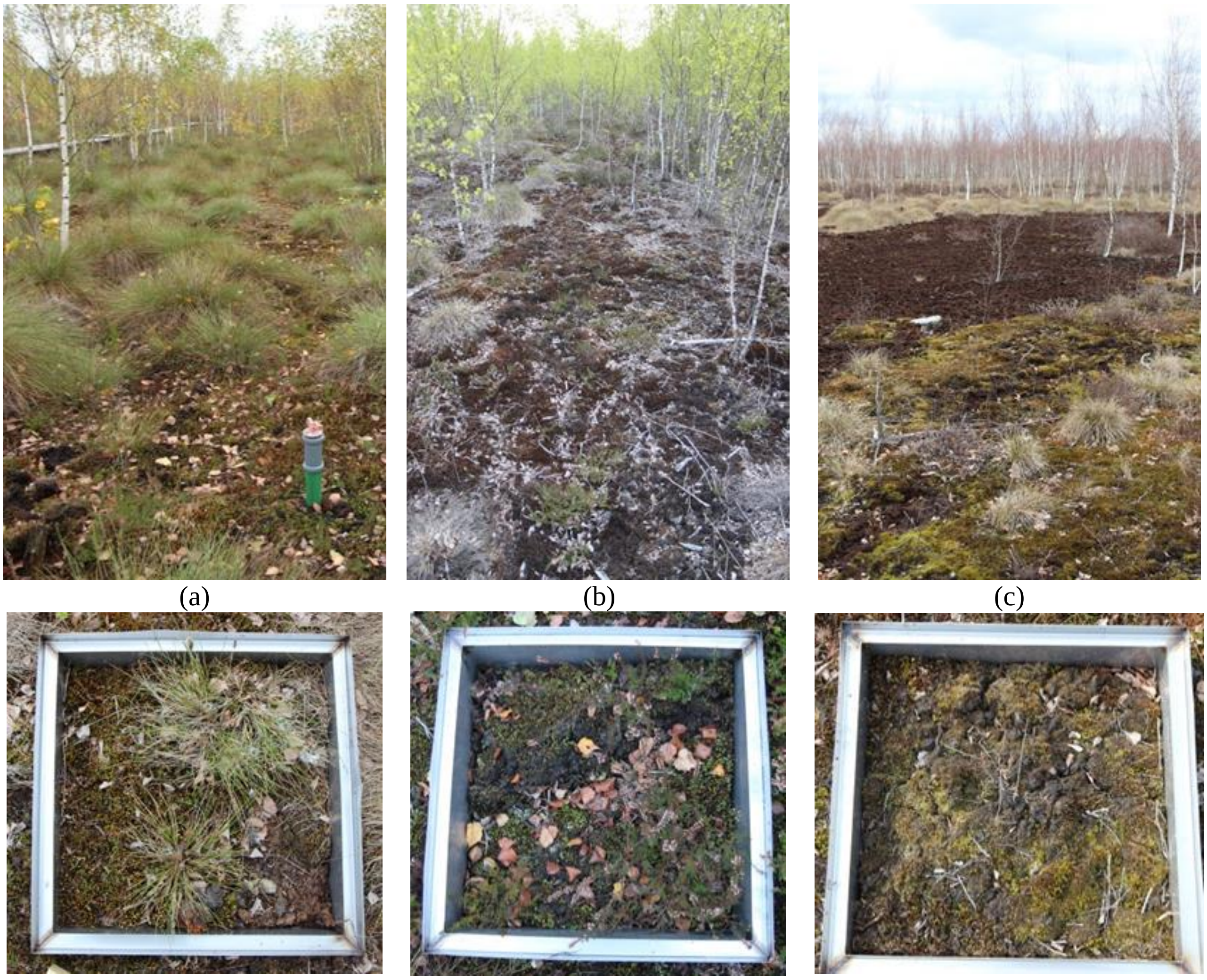

Figure 8. Study sites and research plots illustrating the occurrence of similar structural elements (patches of bare peat with *Polytrichum*) within different 'plant community categories' (considered as potential GESTs): (a) 'sparse birch regrowth with *Eriophorum*', (b) 'post-fire birch stand', (c) 'open areas with bare peat' (photos: M. Napreenko).

of regional validity for the outcomes that may vary between different regions. For this reason, the GHG flux values assigned to 'vegetation forms' (GEST approach) or 'vegetation patches' (vegetation-water level approach) in one location must be adequately calibrated for similar vegetation units elsewhere by field survey that complies with unified criteria. Thus, each case study of peatland vegetation cover could be incorporated into a regional classification of 'vegetation units' (expressed in a way that is compatible with assignment of GHG flux values) that contributes to a general classification for the European temperate zone. This would coincide with carbon supersite goals, which include the testing of technology for GHG balance monitoring (MSHE 2022). Therefore, we envisage our vegetation mapping in the Vittgirrensky Peatland as a site-specific study that could (with potential upscaling) contribute to regional calibrations for both the GEST method and the 'vegetation-water level' approach.


(a) (b) (c) (d) (e) (f)

Figure 9. Drainage ditches in the Vittgirrensky peatland with different vegetation cover (considered as different 'vegetation forms'): (a) with *Eriophorum vaginatum* and *Sphagnum cuspidatum*, (b) with *Typha latifolia* and *Sphagnum spp.*, (c) with *Eriophorum polystachyon* and *Sphagnum angustifolium*, (d) with *Juncus effusus*, (e) with open water and sparse hydrophilic plants, (f) with *Carex rostrata* (photos: M. Napreenko).

ACKNOWLEDGEMENTS

The research was funded by the State Assignment of the Ministry of Science and Higher Education of the Russian Federation, theme No. FZWM-2021-0013. The manuscript was prepared with support from the project 'Restoring Peatlands in Russia - for fire prevention and climate change mitigation' financed under the International Climate Initiative (IKI) of the German Federal Ministry for the Environment, Nature Conservation and Nuclear Safety (BMU), facilitated through the German Development Bank KfW and implemented by Wetlands International in partnership with the Institute of Forest Science, Russian Academy of Sciences, the Michael Succow Foundation and Greifswald University in cooperation with the Ministry of Natural Resources and Environment of the Russian Federation. The authors thank the anonymous reviewers of earlier versions for their valuable comments and suggestions. We are also grateful to Olivia Bragg for editing the manscript and improving the English text.

AUTHOR CONTRIBUTIONS

Conceptualisation: MN and TN-D; methodology: MN and AD; software: AD; investigation, formal analysis and visualisation: MN, TN-D and AD; data curation: MN; writing (preparation of original draft) MN and AD; writing (review and editing): MN, TN-D, AS and AD; supervision: MN. All authors have read and agreed to the published version of the manuscript.

REFERENCES

Alexandrova, V.D. (1969) *Klassifikatsiya rastitel'nosti. Obzor printsipov klassifikatsii i klassifikatsionnykh sistem v raznykh geobotanicheskikh shkolakh* (*Classification of Vegetation: A Review of Classification Principles and Classification Systems at Various Phytocoenological Schools*). Nauka, Leningrad, 275 pp. (in Russian).

Alexandrova, V.D. (1971) K istorii ponyatiya assotsiatsii v geobotanike (On the history of the concept of plant association in geobotany). In: Alexandrova, V.D. (ed.) *Metody vydeleniya rastitel'nykh assotsiatsiy* (*Techniques for Distinguishing Plant Associations*), Nauka, Leningrad, 5–13 (in Russian).

Braun-Blanquet, J. (1964) *Pflanzensoziologie. Grundzuge der Vegetationskunde* (*Plant Sociology: Fundamentals of Vegetation Science*). Springer-Verlag, Vienna - New York, 865 pp. (in German).

Clapuyt, F., Vanacker, V., van Oost, K. (2016) Reproducibility of UAV-based earth topography reconstructions based on Structure-from-Motion algorithms. *Geomorphology*, 260, 4–15. doi: 10.1016/j.geomorph.2015.05.011

Couwenberg, J. (2011) Vegetation as proxy for greenhouse gas fluxes - the GEST approach. In: Tanneberger F., Wichtmann W. (ed.) *Carbon Credits from Peatland Rewetting: Climate - Biodiversity - Land Use*, Schweizerbart, Stuttgart, 37–42.

Couwenberg, J., Augustin, J., Michaelis, D., Joosten, H. (2008) *Emission Reduction from Rewetting of Peatlands. Towards a Field Guide for the Assessment of Greenhouse Gas Emission from Central European Peatlands*. Duene/RSPB, Greifswald/Sandy, 29 pp.

Couwenberg, J., Thiele, A., Tanneberger, F., Augustin, J., Bärisch, S., Dubovik, D., Lyashchynskaya, N.V., Michaelis, D., Minke M., Skuratovich, A., Joosten, H. (2011) Assessing greenhouse gas emission from peatlands using vegetation as a proxy. *Hydrobiologia*, 674, 67–89.

Daniels, R.E., Eddy, A. (1985) *Handbook of European Sphagna*. Institute of Terrestrial Ecology, Huntingdon, UK, 262 pp.

Dierßen, K. (1996) *Bestimmungsschlüssel der Torfmoose in Norddeutschland* (*Key to the Identification of Peat Mosses in Northern Germany*). Mitteilungen der Arbeitsgemeinschaft Geobotanik in Schleswig-Holstein und Hamburg 50, 86 pp. (in German).

Ellenberg, H., Weber, H.E., Düll, R., Wirth, V., Werner, W., Paulißen, D. (1992) *Zeigerwerte von Pflanzen in Mitteleuropa* (*Indicator Values of Plants in Central Europe*). Scripta Geobotanica 18, Verlag Erich Goltze, Göttingen, 258 pp. (in German).

Google Maps (2020) Satellite imagery of the Vittgirrensky peatland. Online at: https://goo.gl/maps/PZf4MZRFbKKPXa3p6, retrieved 15 Dec 2020.

Grummo, D.G., Zelenkyevich, N.A., Sozinov, O.V., Broska, T.V. (2009) Rastitel'nost' verkhovykh bolot Belarusi: geografiya, kartografirovaniye, klassifikatsiya i okhrana (Vegetation of raised bogs in Belarus: geography, mapping, classification and conservation). In: *Vegetation of Mires: Modern Problems of Classification, Mapping, Use and Protection*, Proceedings of the International Theoretical and Practical Seminar, Minsk, Belarus, 127–137 (in Russian).

Ignatov, M.S., Ignatova, E.A. (2003) *Moss Flora of Middle European Russia. Volume 1: Sphagnaceae - Hedwigiaceae*. Arctoa 11, suppl. 1, Moscow, 608 pp. (in Russian with English summary).

Jeschke, L., Knapp, H.D., Succow, M. (2001) Moorregionen Europas. In: Succow, M., Joosten, H. (eds.) *Landschaftsökologische Moorkunde* (*Landscape Ecology of Mires*), Schweizerbart, Stuttgart, 256–316 (in German).

Jiroušek, M., Peterka, T., Chytrý, M., Jiménez-Alfaro, B. and 36 others (2022) Classification of European bog vegetation of the *Oxycocco-Sphagnetea* class. *Applied Vegetation Science*., 25, e12646, 19 pp. doi: 10.1111/avsc.12646

Joosten, H. (2009) *The Global Peatland CO_2 Picture. Peatland Status and Emission in All Countries of the World*, Wetlands International, Ede, Netherlands, 35 pp.

Joosten, H., Tapio-Biström, M.-L., Tol, S. (2012) *Peatland - Guidance for Climate Change Mitigation Through Conservation, Rehabilitation and Sustainable Use*. FAO and Wetlands International, Rome, 100 pp.

Katz, N.Ya. (1971) *Bolota zemnogo shara (Mires of the World)*. Nauka, Moscow, 295 pp. (in Russian).

Koska, I., Succow, M., Clausnitzer, U., Timmermann, T., Roth, S. (2001) Vegetationskundliche Kennzeichnungen von Mooren (topische Betrachtung). In: Succow, M., Joosten, H. (ed.) *Landschaftsökologische Moorkunde* (*Landscape Ecology of Mires*), Schweizerbart, Stuttgart, 112–184 (in German).

Liu, W., Grootjans, A., Everts, H., Fritz, C., de Vries, N. (2020) Estimation of greenhouse gas emission reductions based on vegetation changes after rewetting in Drentsche Aa brook valley. *Mires and Peat*, 26, 02, 14 pp.

MSHE (2022) Carbon Supersites: Russian Federation. Web page, Ministry of Science and Higher Education of the Russian Federation. Online at: https://carbon-polygons.ru/en/, accessed 20 Apr 2023.

Napreenko, M.G. (2002) *Flora i rastitel'nost' verkhovykh bolot Kaliningradskoy oblasti* (*Flora and Vegetation of Raised Bogs in Kaliningrad Region*). PhD thesis, Immanuel Kant Baltic Federal University, Kaliningrad, 291 pp. (in Russian).

Napreenko, M.G. (2015) Bolotnyye ekosistemy (Mire ecosystems). In: Medvedev, V.A. (ed.) *Priroda Kaliningradskoy oblasti. Vodnyye ob'yekty* (*Nature in Kaliningrad Region: Water Objects*). Istok, Kaliningrad, 56–76 (in Russian).

Napreenko, M.G., Napreenko-Dorokhova, T.V. (2020) The main patterns of present-day zonal vegetation development in Kaliningrad Oblast, Russian Federation (southeastern Baltic), inferred by palynological data. *Vestnik of Saint Petersburg University: Earth Sciences*, 65(2), 337–361 (in Russian with English summary). doi: 10.21638/spbu07. 2020.207

Napreenko, M.G., Antsiferova, O.A., Aldushina, Y.K., Baranovskiy, P.N., Aldushin, A.V., Samerkhanova, A.K., Tumilovich, O.A., Kesoretskikh, I.I. (2018) *Obsledovaniye narushennykh torfyanykh bolot na territorii Kaliningradskoy oblasti s tsel'yu vosstanovleniya bolotnykh ekosistem* (*Investigations in the Human-disturbed Peatlands in the Kaliningrad Region for the Purposes of Mire Ecosystem Rehabilitation*). report on the scientific research project WWF951/RU005648/GLO, Natural Heritage, Kaliningrad, 111 pp. (in Russian).

Napreenko, M.G., Antsiferova, O.A., Aldushin, A.V., Samerkhanova, A.K., Aldushina, Y.K., Baranovskiy, P.N., Napreenko-Dorokhova, T.V., Panov, V.V., Konshu, E.V. (2021) New approaches to sustainable management of wetland and forest ecosystems as a response to changing socio-economic development contexts. In: Leal Filho, W., Krasnov, E.V., Gaeva, D.V. (eds.) *Innovations and Traditions for Sustainable Development*, World Sustainability Series, Springer, Cham, Switzerland, 395–416. doi: 10.1007/978-3-030-78825-4

Neitzel, F., Klonowski, J. (2011) Mobile 3D mapping with a low-cost UAV system. *The International Archives of the Photogrammetry, Remote Sensing and Spatial Information Sciences*, XXXVIII-1/C22, 39–44.

Nocerino, E., Menna, F., Remondino, F., Lunazzi, R.S. (2013) Accuracy and block deformation analysis in automatic UAV and terrestrial photogrammetry - lesson learnt. In: Grussenmeyer, P. (ed.) *ISPRS Annals: XXIV International CIPA Symposium (Vol. II–5/W1)*, International Society for Photogrammetry and Remote Sensing, Strasbourg, France, 203–208. doi: 10.5194/isprsannals-II-5-W1-203-2013

Orlyonok, V.V. (ed.) (2008) *Geografiya Yantarnogo kraya Rossii* (*Geography of the Amber Region of Russia*). Yantarnyi Skaz, Kaliningrad, 424 pp. (in Russian).

Premke, K., Attermeyer, K., Augustin, J., Cabezas, A., Casper, P., Deumlich, D., Jörg Gelbrecht, J., Horst, H., Gerke, H.H., Gessler, A., Grossart, H.-P., Hilt, S., Hupfer, M., Kalettka, T., Kayler, Z., Lischeid, G., Sommer, M., Zak, D. (2016) The importance of landscape diversity for carbon fluxes at the landscape level: small-scale heterogeneity matters. *Wiley Interdisciplinary Reviews: Water*, 3, 601–617. doi: 10.1002/wat2.1147

Rivas-Martínez, S., Rivas-Sáenz, S., Penaz, A. (2011) Worldwide bioclimatic classification system. *Global Geobotany*, 1, 1–634. doi: 10.5616/gg110001

Schwill, S., Haberl, A., Strauss, A. (2010a) *Greenhouse Gas Emission of Peatlands. Methodology for the Assessment of Climate Relevance - Case Study Zehlau Peatland*. Michael Succow Stiftung, Greifswald, Germany, 18 pp.

Schwill, S., Strauss, A., Napreenko, M., Gusev, W., Haberl, A. (2010b) *100 Jahre Zehlau - Klimarelevanz eines Hochmoores in Kaliningrad, Russland* (*100 years of Zehlau - Climate Relevance of a Raised Bog in Kaliningrad, Russia*). Final report, Project No. (FKC) 380 01 217, Michael Succow Stiftung, Greifswald, 64 pp. (in German).

Sirin, A.A., Suvorov, G.G., Chistotin, M.V., Glagolev, M.V. (2012) Values of methane emission from drainage ditches. *Environmental Dynamics and Global Climate Change*, 3(2), 1–10 (in Russian with English summary). doi: 10.17816/edgcc321-10

Sirin, A.A., Medvedeva, M.A., Maslov, A.A., Vozbrannaya, A.E. (2018) Assessing the land and vegetation cover of abandoned fire hazardous and rewetted peatlands: comparing different multispectral satellite data. *Land*, 7(2), 71, 22 pp. doi: 10.3390/land7020071

Sirin, A.A., Medvedeva, M.A., Makarov, D.A., Maslov, A.A., Joosten, H. (2020) Monitoring of vegetation cover of rewetted peatlands in Moscow Oblast. *Vestnik of Saint Petersburg University: Earth Sciences*, 65(2), 337–361 (in Russian). doi: 10.21638/spbu07.2020.206

Snavely, N., Seitz, S.M., Szeliski, R. (2008) Modeling the world from internet photo collections. *International Journal of Computer Vision*, 80, 189–210. doi: 10.1007/s11263-007-0107-3

The Rosyanka (2022) Karbonovyj poligon 'Rosyanka': Nauchno-obrazovatel'nyi proyekt po izucheniyu klimaticheski aktivnykh parnikovykh gazov (The Rosyanka Carbon Polygon: Scientific and educational project for the study of active greenhouse gases). Website (in Russian). Online at: http://rosyanka.kantiana.ru/#rec329995215, accessed 30 Aug 2022.

Tiele, A., Minke, M.C., Leshchinskaya, N.V., Tanneberger, F., Joosten, H. (2009) Vegetation types and mean water level fluctuations as a proxy for greenhouse gas emission. In: *Vegetation of Mires: Modern Problems of Classification, Mapping, Use and Protection*, Proceedings of the International Theoretical and Practical Seminar, Minsk, Belarus, 236–241.

Waddington, J.M., Day, S.M. (2007) Methane emission from a peatland following restoration. *Journal of Geophysical Research*, 112, e12646, 11 pp. doi: 10.1029/2007JG000400

Yurkovskaya, T.K. (1980) Bolota (Mires). In: Gribova, S.A., Isachenko, T.I., Lavrenko, E.M. (eds.) *Rastitel'nost' evropeyskoy chasti SSSR* (*Vegetation of the European Part of the USSR*), Nauka, Leningrad, 300–345 (in Russian).

Submitted 22 Nov 2022, final revision 25 Aug 2023
Editors: Mike Peacock and Olivia Bragg

Author for correspondence:
Dr Maxim Napreenko, Immanuel Kant Baltic Federal University, 14 A. Nevskogo str., 236016 Kaliningrad, Russia. Tel: +79211072797; E-mail: maxnapr@gmail.com

Appendix

Table A1. Floristic composition of different Plant Community Categories compiled on the basis of relevés recorded in the Vittgirrensky Peatland. The categories are numbered according the vegetation map (Figure 5). The Roman numerals I–V indicate frequency classes. The indices 1–5, + and ‘r’ are scores on the Braun-Blanquet cover-abundance scale.

Species name	**Plant Community Category**																				
	1	**2**	**3**	**4**	**5**	**6**	**7**	**8**	**9**	**10**	**11**	**12**	**13**	**14**	**15**	**16**	**17**	**18**	**19**	**20**	**21**
Arboreal species																					
Betula pendula	V$^{2-3}$	IV$^{1-4}$	V$^{2-5}$	V$^{4-5}$	V$^{2-3}$	V$^{1-2}$	V$^{3-4}$	V^{5}	V$^{3-4}$	V$^{1-3}$	V$^{4-5}$	V$^{2-3}$	V^{1}	IV^{+-2}	IV^{+-1}	II^{+}		V^{1}	III^{+}	IV^{+}	
B. pendula (regrowth)				III^{1}							V$^{3-4}$	V$^{1-2}$		II^{+}			II^{+}	V^{1}			II^{+}
B. pubescens				III^{+}	V^{1}	III^{+}	III^{+}		III^{1}	III^{1}		III^{+}		III^{+}	II^{+}		I^{+}	III^{+}	I^{+}		
B. pubescens (regrowth)				III^{+}													II^{+}				II^{+}
Corylus avellana	III^{+}	II^{1}																			
Crataegus monogyna	V^{+-1}	V$^{2-3}$	II^{1}													II^{+}					
C. monogyna (regrowth)				IV^{+}												II^{+}					
Euonymus europaeus	II^{+}																				
Frangula alnus		III^{+-2}													IV^{+-1}	I^{+}					
F. alnus (sprouts)	II^{+}													III^{+}	IV^{+}						
Padus racemosa	II^{+}																				
Picea abies						I^{+}															
Pinus sylvestris				II^{+}	II^{+}	II^{+}	IV^{+}	I^{+}	V^{3}			IV^{+}	II^{+}					I^{+}			I^{r}
Populus tremula	V^{3}	IV$^{1-4}$	V^{+}	V^{+-1}			III^{+}					II^{+}									
P. tremula (regrowth)	III^{+}				II^{1}	II^{1}				III^{1}	I^{+}	II^{1}	III^{+}								
Quercus robur	III^{+-1}																				
Q. robur (sprouts)	III^{r}			I^{r}			II^{r}		IV^{+}			I^{r}				I^{+}					
Ribes rubrum	II^{+}																				
Salix aurita												III^{+}	III^{+}	V^{+-1}	IV^{+}	II^{+}	IV^{+}	III^{+}			
S. caprea	III^{3}			II^{+}	I^{r}					I^{+}											
S. cinerea	II^{+}		II^{1}	III^{+}		II^{+}					II^{+}	IV^{+-1}	IV^{+}	V$^{3-5}$	V$^{3-4}$	V$^{4-5}$	V$^{1-4}$	V$^{1-4}$	IV$^{3-4}$	IV^{1}	I^{r}
S. fragilis																II^{1}					
S. × multinervis (?)						II^{+}							II^{+}								
S. myrsinifolia														III^{+}	IV^{+}						
S. pentandra												I^{+}		IV^{+}	IV^{+}		II^{+}	V$^{1-2}$		III^{1}	

Species name	**Plant Community Category**																				
	1	**2**	**3**	**4**	**5**	**6**	**7**	**8**	**9**	**10**	**11**	**12**	**13**	**14**	**15**	**16**	**17**	**18**	**19**	**20**	**21**
S. purpurea															I^{r}						
S. rosmarinifolia														III^{+}	III^{+-1}						
Sambucus racemosa	II^{+}			I^{+}																	
Sorbus aucuparia	V^{+-1}	V$^{1-2}$	II^{+}	II^{+}																	
Tilia cordata (regrowth)	II^{+}	III^{1}																			
Viburnum opulus		II^{1}													III^{+}						
Suppressed trees															V^{1}						
Vascular plants (herbaceous)																					
Aegopodium podagraria		II^{3}																			
Agrostis canina				I^{+}												II^{1}					
Alisma plantago-aquatica																	II^{+}				
Arctium tomentosum		II^{+}																			
Athyrium filix-femina	III^{+-3}																				
Brachypodium sylvaticum	II^{+}																				
Calamagrostis canescens					I^{+}	II^{+}				II^{+}	II^{+}	III^{+-1}		V$^{1-3}$	V^{1}	II^{3}	V^{+-4}	IV^{+-4}	III^{+}	V^{4}	
C. epigeios				IV$^{2-3}$							I^{+}				I^{r}						
Callitriche palustris														III^{+}				II^{+}			
Calluna vulgaris				III^{+}	V^{1}	V$^{3-5}$	V$^{3-5}$	V^{+-1}	V^{2}	V$^{1-5}$	III^{1}	IV^{+-2}	V$^{4-5}$					II^{+}			I^{+}
Calystegia sepium																II^{+}					
Cardamine amara																II^{+}					
Carex acuta																		III$^{1-3}$	III^{+}		
C. canescens	I^{+}																				
C. digitata															II^{+}						
C. flava															III^{+-1}					II^{+}	
C. lasiocarpa															III$^{1-4}$						
C. lepidocarpa														II^{+}	II^{1}						
C. nigra	I^{+}																				
C. panicea															III^{+-1}						
C. pilulifera														III^{3}	III^{2}						
C. pseudocyperus												I^{+}					II^{+}	IV^{1}		II^{+}	
C. rostrata					I^{1}	III^{+}						III^{+}		III^{+-1}	III^{+-2}		II^{1}	V$^{1-2}$	II^{+}		

Species name	Plant Community Category																				
	1	**2**	**3**	**4**	**5**	**6**	**7**	**8**	**9**	**10**	**11**	**12**	**13**	**14**	**15**	**16**	**17**	**18**	**19**	**20**	**21**
Chamaenerion angustifolium				IV^{+}																	
Circaea lutetiana			II^{+}																		
Cirsium palustre															I^{r}						
C. rivulare														I^{r}	IV^{+}				II^{+}	II^{+}	
Comarum palustre														II^{1}	IV^{+-1}		II^{1}				
Conyza canadensis				II^{1}																	
Drosera rotundifolia					II^{r-1}	+-1						IV^{+-1}	II^{+}				I^{+}	II^{+-1}			
Dryopteris carthusiana	III^{+}	II^{+}										I^{+}		I^{r}							
D. filix-mas	II^{1}	III$^{1-2}$												I^{r}							
Epilobium palustre												I^{+}		III^{+}			II^{+}	II^{+}	III^{+}		
Epipactis helleborine		II^{+}																			
Equisetum fluviatile														III^{+}	III^{+}			II^{+}			
Eriophorum polystachyon															II^{+}						
E. vaginatum				III^{1}	V$^{3-5}$	IV^{2}	V$^{2-3}$	III^{+-1}	V^{2}	V^{+-1}	III^{2}	V$^{3-5}$	V^{1}				V$^{1-2}$	V$^{2-3}$			III^{+}
Eupatorium cannabinum															III^{+}	II^{+}				I^{+}	
Filipendula ulmaria																			II^{+}		
Fragaria vesca	III^{1}	III^{1}	III^{1}	II^{1}																	
Galium palustre																II^{+}					
Hieracium pilosella				I^{r}																	
H. umbellatum	I^{r}																				I^{r}
Humulus lupulus	II^{+}	III^{+-1}																			
Iris pseudacorus	I^{+}																				
Juncus effusus				I^{+}	I^{+}	V^{+-1}					II^{1}	V^{+-2}		II^{+}	III^{+}		V^{3}	IV^{1}	III^{+}	III^{+}	
Ledum palustre				I^{+}	III^{+}	III^{+}	V^{1}		II^{+}			III^{+-1}						I^{+}			
Lemna minor																		III^{+}			
Lycopodium annotinum				I^{+}																	
L. clavatum		I^{r}		I^{r}																	
Lycopus europaeus															III^{+}	II^{+}		II^{+}			
Lysimachia nummularia	II^{+}	III^{1}																			
L. vulgaris			II^{+}	III^{+-1}										III^{+-1}	IV^{1}	II^{1}	IV^{+}	III^{+}	III^{+}	III^{+}	
Lythrum salicaria												I^{+}					II^{+}	II^{+}	III^{+}	III^{+}	
Majanthemum bifolium		II^{1}																			
Moehringia trinervia				II^{+}																	

Species name	**Plant Community Category**																				
	1	**2**	**3**	**4**	**5**	**6**	**7**	**8**	**9**	**10**	**11**	**12**	**13**	**14**	**15**	**16**	**17**	**18**	**19**	**20**	**21**
Phalacroloma annuum				II^{+}																	
Phragmites australis			III^{3}			III^{1}				III^{2}	V^{4}	V$^{2-5}$	V$^{2-3}$	V$^{1-3}$	V$^{1-2}$	II^{+-1}	I^{+}	V$^{1-2}$	V$^{3-5}$	V$^{4-5}$	
Platanthera chlorantha	I^{r}																				
Poa palustris														II^{+}							
Potentilla erecta															II^{+}						
Rubus caesius	II^{1}																				
R. chamaemorus						I^{r}															
R. idaeus		III^{1}	III^{1}	II^{+}																	
Rumex acetosella				I^{+}																	
Scirpus sylvaticus																		I^{+}			
Solanum dulcamara														II^{+}		II^{+}			IV^{+}		
Solidago canadensis		III^{1}	IV$^{1-4}$	+										III^{+}	III^{+}	IV^{+-1}			IV^{+}	II^{2}	
S. virgaurea		II^{+}																			
Tanacetum vulgare				III^{+}																	
Thelypteris palustris												I^{+}		III^{+}				II^{+}			
Typha latifolia																	II^{+}				
Urtica dioica	I^{+}	II^{+}														II^{+}					
Utricularia minor																		II^{1}			
Valeriana officinalis														II^{+}						II^{+}	
Mosses																					
Amblystegium sp.					I^{r}									II^{+}		V^{+-1}	II^{1}		III^{+}	II^{+}	
Atrichum undulatum	II^{+}	IV^{+}																			
Aulacomnium androgynum								IV^{1}	V^{+}			II^{1}									
A. palustre						II^{+}						II^{+}		III^{+-1}			III^{1}	IV^{1}			
Brachythecium sp.	IV^{1}	III^{+}	III^{+}	I^{+}		I^{+}			II^{+}			II+		III^{+}						I^{+}	
Calliergonella cuspidata												I^{+}		IV$^{1-3}$	V^{2}		II^{2}	III$^{1-2}$	III^{3}		
Campylopus introflexus				III^{+}	III^{+-1}	III^{1}	V^{+}			III^{1}	II^{+}	II^{+}	V^{1}								IV^{+-3}
Climacium dendroides	II^{+}													IV^{2}					II^{+}		
Dicranella heteromalla								III^{+}													
Dicranum bergeri						I^{+}															
D. polysetum						II^{+}			III^{1}			I^{+}									

Species name	**Plant Community Category**																				
	1	**2**	**3**	**4**	**5**	**6**	**7**	**8**	**9**	**10**	**11**	**12**	**13**	**14**	**15**	**16**	**17**	**18**	**19**	**20**	**21**
D. scoparium									II^{+}												
Eurhynchium angustirete	III^{1}	II^{+}																			
Herzogiella seligeri				II^{+}																	
Hylocomium splendens									III^{+}												
Hypnum cupressiforme	III^{1}					I^{+}								II^{+}		II^{+}					
Mnium hornum															IV^{+}			II^{+}		II^{r}	
Orthotrichum sp.	III^{1}															IV^{+}					
Plagiomnium affine	II^{+}																				
P. cuspidatum																I^{r}				I^{r}	
P. undulatum		II^{2}																			
Platygyrium repens	II^{1}															II^{+}					
Pleurozium schreberi		II^{+}				II^{+}	IV^{+}	IV$^{1-2}$	V^{+-2}	II^{+}	III^{1}	III^{+}						II^{+}			
Pohlia nutans					IV^{+-1}	II^{+}				III^{+}		I^{+}									
Polytrichum commune	III^{+}							IV^{2}	II^{+}		IV$^{1-2}$	III^{+-2}		II^{1}			IV^{1}	II^{+}	III^{+}		
P. juniperinum				III^{+-1}							II^{+}										
P. strictum					V$^{1-5}$	V^{+-5}	V$^{1-2}$	V$^{1-2}$	V$^{1-2}$	V$^{2-4}$	IV$^{1-2}$	IV$^{1-2}$						II^{+}			
Ptilium crista-castrensis									II^{+}												
Rhytidiadelphus triquetrus	III^{1}																				
Sphagnum angustifolium					II^{+}						II^{+}	III^{+-1}		IV$^{1-2}$			V$^{2-3}$	II^{+-3}			
S. capillifolium					II^{+}	II^{+}	III^{+}		II^{+}		III^{+}	III^{+-1}	II^{+}				II^{2}	II^{+}			
S. centrale												IV^{+-2}					V^{+}				
S. cuspidatum																	V^{+-4}	II$^{1-2}$			
S. fallax	I^{+}	II^{+}			II^{+}																
S. fimbriatum												II^{+}						II^{+-1}			
S. fuscum							I^{+}					III^{+}						II^{+}			
S. magellanicum					II^{+}		II^{+}				II^{+}	III^{+-1}	II^{+}				II^{1}				
S. molle					I^{r}																
S. riparium																	I^{r}				
S. squarrosum	I^{+}											III^{+-1}		III^{1}			V^{+-1}	II^{1}			
S. subsecundum															IV^{+}						
S. teres												I^{1}					II^{1}				
Thuidium tamariscinum	III^{1}																				
Warnstorfia fluitans																	IV$^{1-2}$				

Species name	Plant Community Category																				
	1	2	3	4	5	6	7	8	9	10	11	12	13	14	15	16	17	18	19	20	21
Hepatics																					
Lophozia sp.																	I^{+}				
Marchantia polymorpha																		II^{+}		II^{+}	
Radula complanata	II^{+}																				
Lichens																					
Cladonia chlorophaea				IV^{+}	IV^{+}	III^{+}	V^{+}	V^{+}	V^{+}	V^{+}	IV^{+}	I^{+}	V^{+}								
Cladonia macilenta							IV^{+}														
Cladonia spp.				V^{+}	III^{1}	III^{+}	IV^{1}	IV^{+}	V^{+}	V$^{1-2}$	IV^{+}	I^{+}	V^{+-1}								III^{+}
Hypogymnia physodes	II^{+}	II^{+}	II^{+}		III^{+}	III^{+}	V^{+}	II^{+}	II^{+}	II^{+}	III^{+}	I^{+}	II^{+}			I^{+}	II^{+}	III^{+}			
Parmelia sp.						II^{+}	III^{+}						IV^{+}				IV^{+}				
Peltigera canina	II^{+}			I^{+}																	
Ramalina farinacea	III^{+}					I^{+}	III^{+}										IV^{+}				
Xanthoria parietina	II^{+}																II^{+}				
Fungi																					
Amanita citrina				I^{r}																	
A. fulva				IV^{+}		I^{+}	V^{+}		II^{+}												II^{r}
Clitocybe sp.				I^{r}																	
Collybia dryophila				I^{r}																	
Cortinarius sp.												I^{r}					II^{+}	I^{+}			
Entoloma sp.							I^{r}														
Galerina paludosa																		I^{+}			
Hygrocybe sp.												I^{r}									
Laccaria laccata				I^{r}								I^{r}						I^{r}			
Lactarius vietus				I^{r}		I^{r}	I^{r}			II^{r}	I^{r}		II^{r}				I^{r}	I^{r}			
Marasmius androsaceus				I^{r}			I^{r}					I^{r}									
Mycena vitilis				I^{r}																	
Russula betularum				I^{r}								I^{r}									
R. paludosa						I^{+}	I^{+}		II^{+}												